VISIT Deliverable Report Cover Sheet

Workpackage:	W3
Deliverable number	D3.1
Deliverable name	Reference 980 nm TWL
Lead beneficiary:	IOF
Workpackage leader (name):	IOF
Description writer (name):	Dr. Nikita Yu.Gordeev
Date planned:	29.05.2009
Date finished:	28.05.2009

Deliverable reached ☒ not reached ☐

Deliverable description and summary of achieved results (max. 2400 char.):

Series of the waveguide of 980 nm GaInAs/GaAs quantum well (QW) edge-emitting tilted-wave laser (TWL) have been numerically simulated. In the TWL the wavelength stabilization is based on the coupling of the laser active waveguide cavity to a transparent substrate, or a specially introduced thick epitaxial layer. Series of TWL wafers have been grown by the metal-organic chemical vapour deposition (MOCVD). Basic laser parameters (threshold current, efficiency, intrinsic losses, far-field pattern) have been investigated both in pulsed and CW mode. The complex vertical far-field pattern is defined by the resonance interaction of the two coupled cavities. Electroluminescence measurements have been performed in the temperature range of 15-70°C. The lasers with optimized waveguide design have shown high temperature stability of the lasing wavelength (0.05 nm/K) in the temperature range of 20-50^{0}C under CW excitation, which proves the concept of thermal stability in TWL. The obtained results and reference TWL design will be used for developing tilted wave lasers emitting at 1300 nm.

Contributions:

IOF, VIS

Public

VISIT deliverable report technical annex

1. Introduction

Wavelength stabilization is extremely important in multiple applications, from telecom and datacom transmitters to frequency conversion and solid state laser pumping.

The disadvantage of conventional edge-emitting lasers is the fact that the lasing wavelength is not stabilized and it shifts toward longer wavelengths with temperature increase, reflecting the shrinkage of the semiconductor band-gap.

The temperature dependence of the gain spectrum and lasing wavelength therefore is roughly given by [1, p.114]

$$d l/dT » 1.24\ d(E_g^{-1})/dT$$

$$\approx -1.24\ E_g^{-2}(dE_g/dT)\ , \qquad (1)$$

where E_g is the band-gap energy. Typical temperature coefficient $d l/dT$ is 0.4-0.5 nm/K in the wavelength of 1000-1300 nm.

The different temperature behavior takes place if the lasing wavelength is mainly determined by the laser cavity but not the gain. This situation is realized for instance in VCSEL where DBRs and cavity itself define the lasing wavelength. In this case the temperature dependence of the lasing wavelength follows the temperature dependence of the refractive index [2] and is given by

$$d l/dT » (l/n)\ dn/dT, \qquad (2)$$

where l is the emission wavelength and n is refractive index. The value of dn/dT is between 2×10^{-4} and 5×10^{-4} K^{-1}. Thus the temperature coefficient of the emission wavelength $d l/dT$ is ~ 0.05-0.1 nm/K.

2. Tilted wave laser (TWL) concept

It has been previously shown that it is possible to create edge-emitting lasers where not only the waveguide is involved in lasing. In so-called leaky wave diode lasers [3, 4] lasing is developed within a thin waveguide active region (as in usual edge-emitting diode lasers), while the output emission is emission leaking to a semiconductor substrate.

The Tilted Wave Laser (TWL) concept is based on the existence of the tilted modes originating in planar waveguides with thin cladding layers. The light of these modes is propagating at the leakage angle outside the waveguide and is being reflected back (Fig. 1). This reflection enables lasing in TWL and provides its specific features in particular wavelength thermal stability. The concept of wavelength stabilization in edge–emitting lasers, which is achieved exclusively through epitaxial design was proposed in 2002 [5].

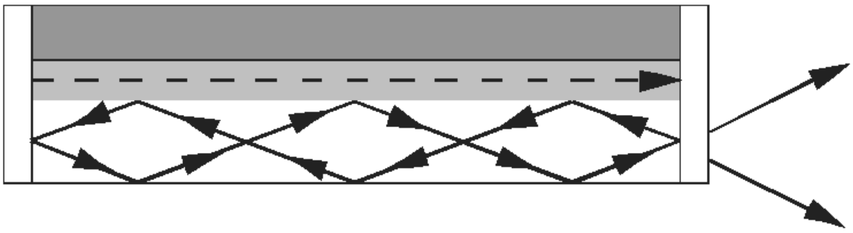

Fig. 1 Sketch of tilted wave laser waveguide.

There are two different approaches for wavelength stabilization using tilted modes. In one case (tilted cavity laser, or TCL), the wavelength selectivity was proposed to be reached by loss engineering in the leaky waveguide layer attached to a narrow stopband Bragg-reflector at a wavelength and leakage angle. At the matching wavelength and angle the leakage is suppressed by the stopband reflectivity. The disadvantage of the TCL approach is in the very large thickness of the epitaxial DBR needed to achieve a sharp minimum in the losses.

In the second approach referred as Tilted Wave Laser (TWL) [6], no leakage loss selectivity is necessary and the wavelength stabilization is realized through phase matching, which occurs only in case of lasing or at least stimulated emission in the device. All the leaky light is reflected in this approach back to the cavity by a single (or multiple) reflection from the underlying layer (layers). Coherent leaky light, passing through multiple reflections accumulates a phase difference and interferes with the light, which is propagating in the planar leaky waveguide. In case the interference is constructive, the phase matching condition is fulfilled and wavelength stabilization is taking place. The easiest approach to realize such a device is to use the back reflection of the leakage emission from the polished substrate backside towards the active zone of the leaky waveguide. The TWL approach thus provides an opportunity to reduce costs of the device in comparison with TCL due to simpler, thinner and much more robust layer architecture.

Comparison of the TWL concept with other concepts for single mode operation of edge emitters is given in Appendix – Single mode lasers.

3. Design issues (modeling)

Optical modes have been simulated by using original codes.

According to the Maxwell equations TE mode propagation in multilayer waveguide is described by

$$\frac{\partial^2 E_x}{\partial x^2} + \left(k^2 n^2(x) - h^2\right) E_x = 0$$
$$E(x,z,t) = E_x \exp(iwt - ihz) \qquad (3)$$

where z is the propagation direction, x is the direction perpendicular to the z direction, k is the wavenumber in vacuum, h is the mode wavenumber, $n(x)$ is the waveguide layer refractive index. Solving of the Eq. 3 for complex optical waveguide may be simplified by proper choice of the boundary conditions. We have used the model of Unaxial Perfectly matched layer (uPML) [7, 8]. The main idea of the model is the replacing boundary layers by specific absorbing PML-layers where the Eq. 3 transforms by the rule

$$\frac{\partial}{\partial x} \to \frac{1}{1 + i\frac{s(x)}{w}} \frac{\partial}{\partial x} , \qquad (4)$$

where $s(x)$ is the conductivity of the PML-layer.

Using PML-layers as boundary conditions allows calculating leaky modes and accelerating simulation process. Solving Eq.3 by finite difference (FD) method leads to finding eigenvalue of large matrix (>1000x1000). The application of shift-and-invert Arnoldi technique [9] has been applied, which makes the FD method more accurate, fast and practical.

As it was mentioned above a common feature of tilted wave lasers is that lasing is developed within a thin waveguide active region, while a coupled thick waveguide is involved on the lasing mode formation. In the other words optical mode tunnels from the thin waveguide into the thick waveguide and vice versa. The tunneling is possible in the only case when optical modes exist in either of the waveguides and their effective refractive indexes are equal. The requirement for the thin waveguide is that it should support only one guided mode. The thick waveguide supports several modes but only one mode effectively coupled to the thin waveguide takes place in lasing.

Two types of TWLs have been simulated. The types differ in their thick waveguide design. In the first type (type A) light leaks from the thin waveguide into the substrate which works as a thick waveguide. In the second type (type B) the coupled thick waveguide is formed by introducing a reflecting layer at the distance of several microns from the thin waveguide (Fig. 2). Refractive index of the reflecting layer should be significantly lower than refractive index of the thick waveguide.

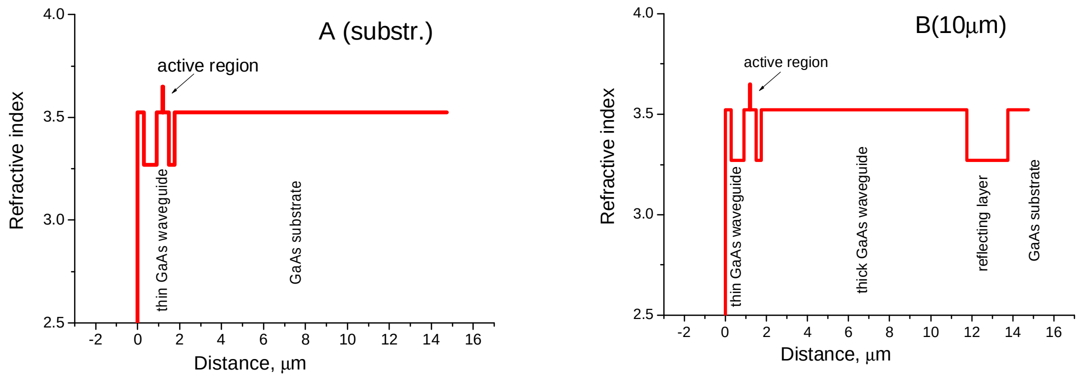

Fig. 2 Two types of TWL: A – without reflecting layer, B – with reflecting layer.

The refractive index and its temperature dependence for the waveguide simulation were calculated according to the Refs. [10, 11, 12].

The most remarkable feature of TWL is vertical far-field pattern. Leaking wave is incident on the cavity facet an angle less than the angle for total internal reflection so the wave emitting from the cavity is angled to the facet normal. In lossless waveguide this leads to forming two narrow lobes in the far-field pattern [13]. Existence of intrinsic losses and gain in leaky laser waveguide may result in redistribution intensity between two lobes. In the TWL of type A where the entire substrate works as a coupled waveguide one lobe almost evanesces. Simulation of near-field pattern and far-field pattern of the TWL of type B is presented in Fig. 3. Two pronounced lobes are clearly seen in the far-field pattern. The intensity in the central part is associated with the light emitting from the thin waveguide. This effect may be eliminated if the feedback in the thin waveguide becomes smaller than the feedback in the coupled thick waveguide.

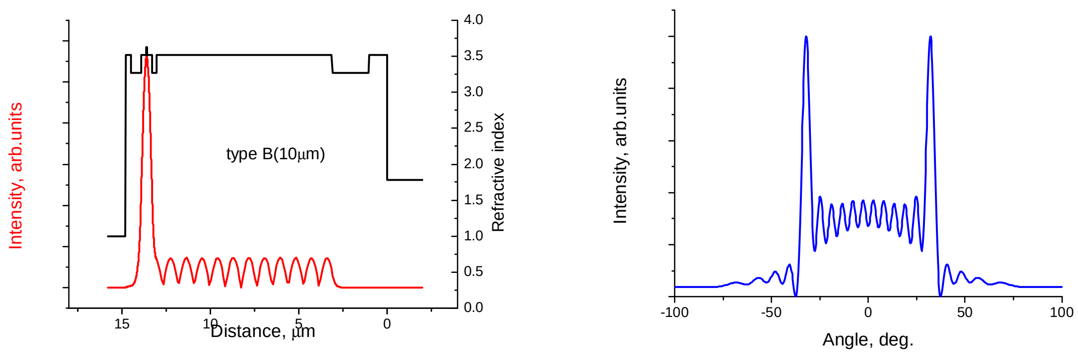

Fig. 3 Simulated near-field pattern (left) and far-field pattern (right) of the TWL of type B.

It is important to notice that the modeling tool calculates optical mode in passive waveguide and does not take into account several specific laser features like current flowing, selfheating etc. In the other word the code used in numerical simulation gives mainly qualitative analysis of the optical mode in TWLs. The real mode behavior is refined by experiment.

4. Epitaxial growth, laser processing and basic laser parameters

Series of the laser wafers were grown by the metal–organic chemical vapour deposition (MOCVD) on *n*-GaAs (100) substrate. The active region and upper part (*p*-part) of the wafers were identical. The active region in all structures consisted of two InGaAs quantum wells inserted into the middle of 0.58 µm thick GaAs waveguide. The structures had 600 nm *p*-GaAsP cladding layer and 300 nm *p*-GaAs contact layer. Lower parts (*n*-part) in the wafers were different. Wafers of type B had 10 µm thick *n*-GaAs coupled waveguide and 2 µm thick *n*-InGaP reflecting layer while the wafers of type A had no these layers. Either of wafer types had *n*-InGaP cladding layer. Thickness of the layer was varied from 200 nm to 400 nm.

After the growth the wafers were processed into 50 µm and 100 µm wide shallow-mesa ridge lasers by etching through the 300 nm p-contact layer. The samples have been used for investigating basic laser parameters. The basic laser parameters such as threshold current density, differential quantum efficiency were measured in pulsed mode (pulse duration 300 ns, repetition frequency 2 kHz). Internal loss and internal quantum efficiency of stimulated emission were determined from the dependence of reciprocal differential quantum efficiency (h_D) on the cavity length (L).

From this point only the TWL wafers showed good laser parameters and thermal stability are described.

Cavity length dependence of threshold current density and lasing wavelength for the TWLs of A and B types are presented in Fig. 4. TWL of type A in spite of free carrier absorption in the substrate shows acceptable value of threshold current density. However, TWL of type B (with reflecting layer) shows significantly lower value of threshold current density – 200 A/cm^2. The lasing wavelength at room temperature lies in the range of 964-1010 nm depending on the wafer and cavity length.

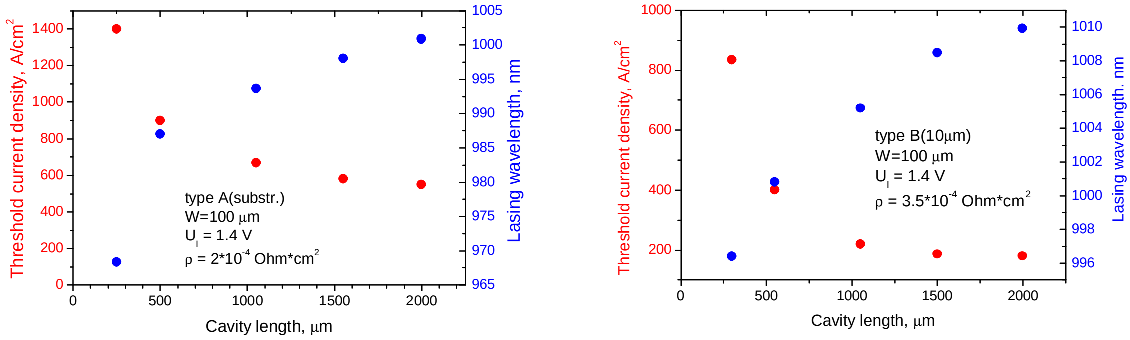

Fig. 4 Dependence of the threshold current density and lasing wavelength on the cavity length for the TWLs of A and B types.

Both types A and B have shown high internal quantum efficiency (Fig. 5) of 90% and 84% respectively. TWL of type A has shown the intrinsic losses of 4.7 cm^{-1}. The value is quite high since in the type A TWL leaky mode propagates through the entire substrate. TWL of type B has shown significantly lower value of intrinsic losses – 2.2 cm^{-1}.

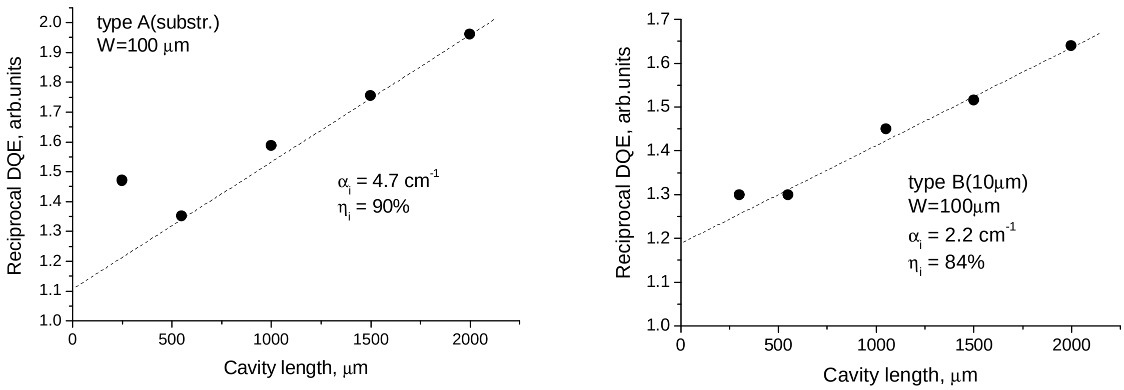

Fig. 5 Dependence of the reciprocal differential quantum efficiency (DQE) on the cavity length for the TWLs of A and B types.

Measured far-field patterns (Fig. 6) qualitatively agree with the far-field patterns obtained in numerical simulations (Fig. 3).

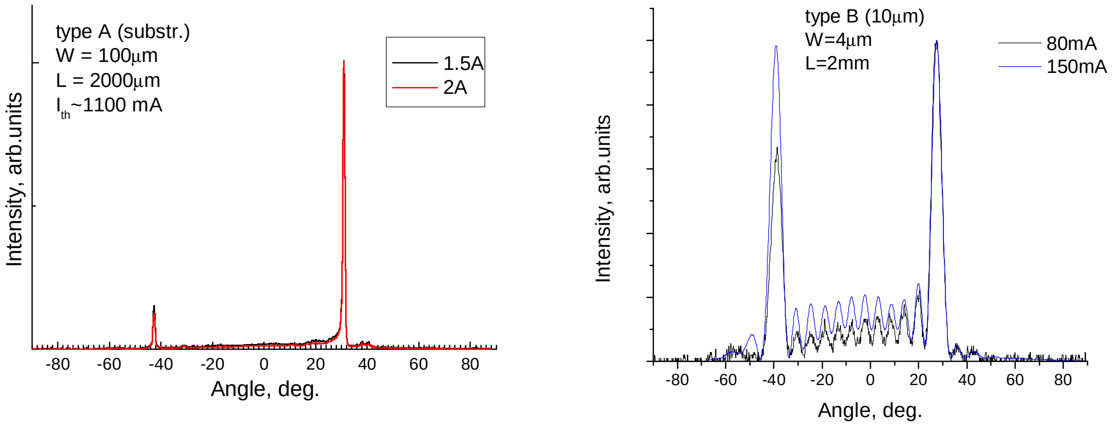

Fig. 6 Far-field patterns.

Summarizing TWLs of type B (with reflecting layer) shows better laser parameters (lower threshold current density, lower intrinsic losses) than TWLs of type A.

5. High temperature stability

The TWL wafer of type B has been processed into 4 μm wide shallow-mesa ridge lasers by etching through the 300 nm p-contact layer and partly through the p-cladding layer (Fig. 7).

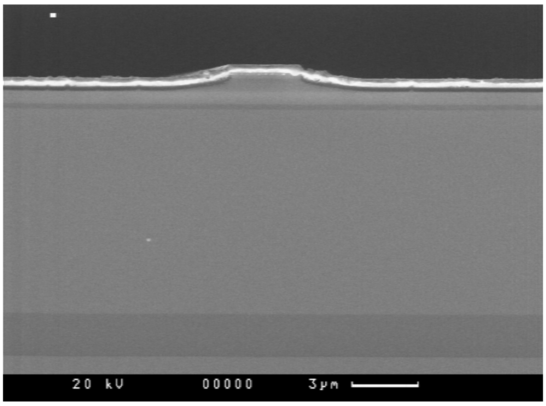

Fig. 7 SEM image of the TWL of type B (stripe width - 4 μm). In the image the reflecting layer is clearly seen.

Lasers were mounted *p*-side down on copper heatsink. The laser parameters were measured in CW mode in the temperature range of 15-60^{0}C.

The lasers operate in fundamental lateral mode that was confirmed by far-field pattern measurements (Fig. 8). Trace of the first-order mode is observed. Lasers operating at longer wavelength should eliminate this effect.

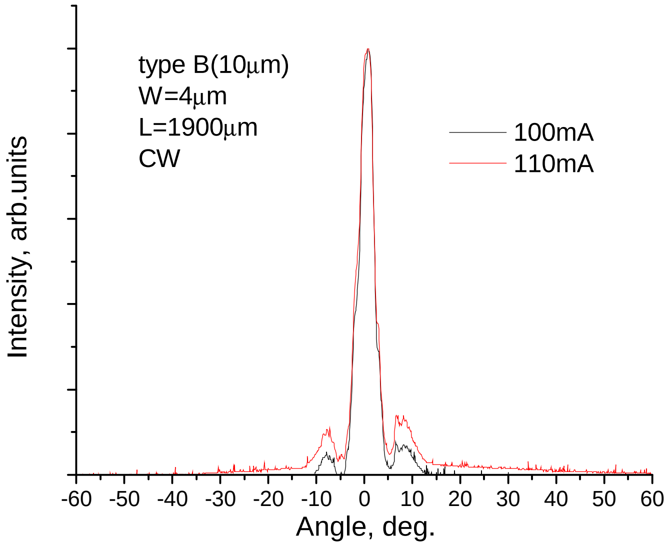

Fig. 8 Lateral far-field pattern.

Fig. 9 shows temperature dependence of L-I curves. Differential quantum efficiency was calculated from this figure. It decreases with increasing the temperature. DQE at room temperature is 83%. Threshold current slightly changes with temperature so estimated value of characteristic temperature T_0 exceeds 500 K.

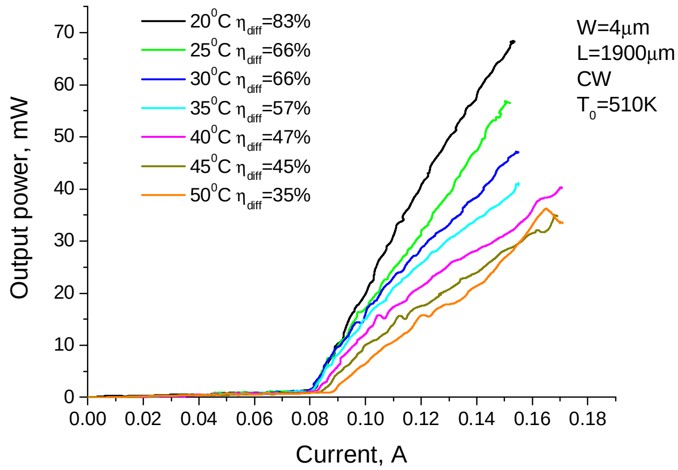

Fig. 9 Temperature dependence of L-I.

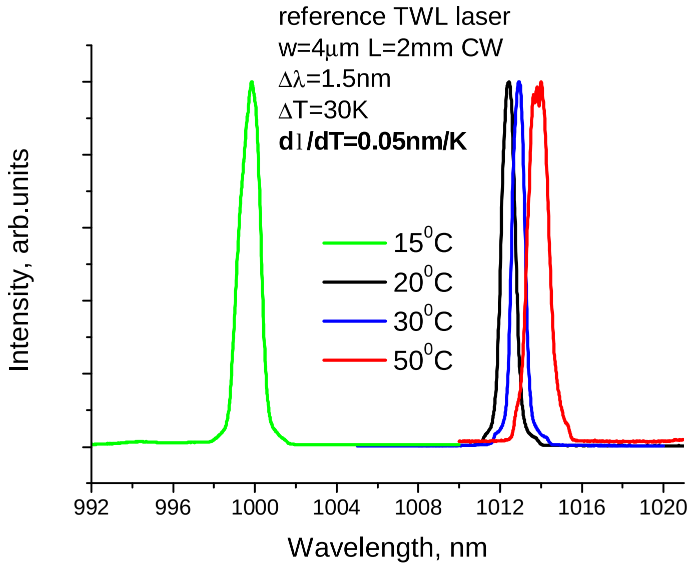

Fig. 10 Lasing spectra temperature dependence.

Fig. 10 shows temperature dependence of the lasing spectra of the TWL of type B. In the range of 20-50^{0}C (ΔT=30K) temperature-induced shift of the lasing wavelength is 1.5 nm, which gives temperature coefficient *dl/dT* of 0.05 nm/K. Beyond this temperature range lasing wavelength is discretely shifted. Wavelength at 15^{0}C is 999.85 nm while at 20^{0}C lasing wavelength is 1012.45 nm. This fact confirms that lasing wavelength is determined by the allowed TWL modes originated from the waveguide coupling [14] and the spectral distance Δλ between the modes is more than 10nm. Lasing in TWL takes place only if the mode wavelength lies within the gain spectrum. Temperature shift of the resonant wavelength of the allowed TWL modes is dominated by *dn/dT* (see Eq.2) and the shift is ~0.05 nm/K. At the same time temperature shift of the gain is ~0.4 nm/K at the 980 nm wavelength (Eq.1). It means that temperature range of high temperature stability is determined by the gain width (Fig. 11) and roughly may be estimated by

$$DT = Dl_G/(dl_G/dT - dl_W/dT) \quad , \qquad (5)$$

where DT is the range of temperature stability, Dl_G is the gain width, dl_G/dT is the temperature dependence of the gain and dl_W/dT is the temperature dependence of the transmission band (wavelength of the optical mode). Thus broader gain spectrum allows increasing the range of temperature stability.

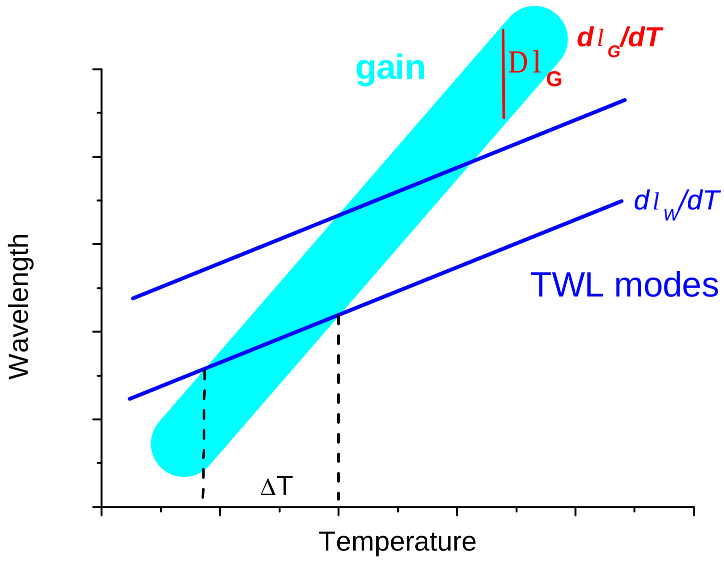

Fig. 11 Temperature range of high temperature stability.

Single transverse mode devices at short cavity lengths are expected to work in a single longitudinal and transverse mode with a high side mode suppression ratio.

EOM TWL concept

Tilted wave laser can be easily integrated vertically with the electro-optically modulated (EOM) section and, thus, operate at ultrahigh speeds.

There are two key features, which enable the functionality of the EOM TWL:

1) Wavelength stabilization

The all epitaxial TWL design enables wavelength-stabilized operation, which is a must both for proper single mode single wavelength DFB-class operation, needed for coupling to single mode fiber and avoiding wavelength dispersion effects, and also a prerequisite for intensity modulation using the electro-optical effect.

2) Vertical Integration

After fabricating a TWL, the vertically-integrated EOM concept will be applied to such a laser. The coupling strength between the thin waveguide and the TWL section is controlled by the EO-modulator media, which is introduced either directly into the narrow coupled waveguide, or adjusted in its vicinity. Now the coupling efficiency can be tuned and the EO-modulated TWL can be realized.

6. Conclusions

Tilted wave laser (TWL) designs have been numerically simulated by original code. Series of 980nm TWL wafers have been grown by MOCVD technique. The wafers were processed into the broad-area and narrow ridge lasers. Basic laser parameters (threshold current, efficiency, intrinsic losses, far-field pattern) have been investigated both in pulsed and CW mode. The complex vertical far-field pattern is defined by the resonance interaction of the two coupled cavities. The lasers with optimized waveguide design have shown high temperature stability of the lasing wavelength (0.05 nm/K) in the temperature range of 20-50^{0}C under CW excitation, which proves the concept of thermal stability in TWL. The obtained results and reference TWL design will be used for developing tilted wave lasers emitting at 1300 nm.

Appendix - Single-mode lasers

I. Introduction

A **single-frequency laser** (sometimes called a *single-wavelength laser*) is a laser which operates on a single resonator mode, so that it emits quasi-monochromatic radiation with a very small linewidth and low phase noise. Because any mode distribution noise is eliminated, single-frequency lasers also have the potential to have very low intensity noise. Particularly in low-power single-frequency lasers such as laser diodes (LDs), there is some small amount of optical power in various resonator modes, even though one mode is clearly dominating. This is because such modes may be only slightly below the laser threshold, so that spontaneous emission can already generate some substantial power. The *mode suppression ratio* (MSR) is then defined as the power of the lasing mode divided by that in the next strongest mode. It can be optimized by making the laser resonator more frequency-selective.

Single-frequency lasers can be very sensitive to optical feedback. Even if less than a millionth of the output power is sent back to the laser, this may in some cases cause strongly increased phase noise and intensity noise or even chaotic multimode operation. Therefore, single-frequency lasers have to be carefully protected against any back-reflections, often using one or two Faraday isolators.

Typical applications of single-frequency lasers occur in the areas of optical metrology (e.g. with fiber-optic sensors) and interferometry, optical data storage, high-resolution spectroscopy (e.g. LIDAR), and optical fiber communications. In some cases such as spectroscopy, the narrow spectral width of the output is directly important. In other cases, such as optical data storage, a low intensity noise is required, thus the absence of any mode beating noise.

Single-frequency sources are also attractive because they can be used for driving resonant enhancement cavities, e.g. for nonlinear frequency conversion, and for coherent beam combining. The latter technique is currently used to develop laser systems with very high output powers and good beam quality.

II. Types of Single-frequency Lasers

In general types of diode edge-emitting single-frequency lasers could be classified by the construction as following:

1) Diode Lasers with the complex optical waveguide construction requiring special processing schemes (DBR, DFB, α-DFB lasers, etc.).

2) Diode External Cavity Lasers.

3) Diode Lasers with the all-epitaxial design (TCL and TWL concepts).

Below different types of the lasers mentioned above are discussed.

1. **Diode Lasers with the complex optical waveguide construction** requiring special processing schemes.

Stable single-mode operation is often achieved with **distributed feedback lasers** (DFB lasers) or **distributed Bragg reflector lasers** (DBR lasers).

1.1 DFB lasers

A distributed-feedback laser [15, 16, 17, 18, 19, 20] is a laser where the whole resonator consists of a periodic structure, which acts as a distributed reflector in the wavelength range of laser action, and contains a gain medium (Fig. 12).

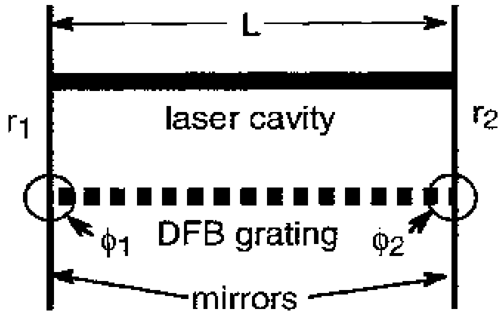

Fig. 12 Schematic of the DFB laser [3].

Typically, the periodic structure is made with a phase shift in its middle. This structure is essentially the direct concatenation of two Bragg gratings with internal optical gain. It has multiple axial resonator modes, but there is typically one mode which is favored in terms of losses. Therefore, single-frequency operation is often easily achieved, despite spatial hole burning due to the standing-wave pattern in the gain medium. Due to the large free spectral range, wavelength tuning without mode hops may be possible over a range of several nanometers. However, the tuning range may not be as large as for a distributed Bragg reflector laser.

Semiconductor DFB lasers can be built with an integrated grating structure, e.g. a corrugated waveguide. Such devices are available in a wide spectral range at least between 0.8 µm and 2.8 µm. Typical output powers are some tens of milliwatts. The linewidth is typically a few hundred MHz, and wavelength tuning is often possible over several nanometers. Temperature-stabilized devices, as used e.g. in DWDM systems, can exhibit a high wavelength stability.

DFB lasers at 1310 nm and 1490 nm on InGaAsP/InP material system [18] wavelength have been designed, fabricated and tested over a wide temperature range. These lasers exhibited good performances such as high reliability, high power, high modulation speed, slow variation of power with temperature, and small tracking error as well.

In [19] first results for high performance monomode quantum dot (QD) DFB laser diodes in the wavelength range of interest are discussed. The spectral gain properties of the underlying QD active region allow realizing DFB lasers with emission spanning an extremely broad wavelength range of 65nm ranging from around 1095nm to 1160nm based on the identical laser structure.

1.2 DBR lasers

A distributed Bragg reflector laser [21, 22, 23, 24, 25, 26, 27, 28, 29, 30] is a laser, where the laser resonator is made with at least one distributed Bragg reflector (DBR) outside the gain medium (the active region). A DBR is a Bragg mirror, i.e., a light-reflecting device (a mirror) based on Bragg reflection at a periodic structure (Fig. 13). In most cases, the Bragg mirror is more specifically a quarter-wave mirror, providing the maximum amount of reflection for the given number of layers.

Examples of the DBR laser constructions:

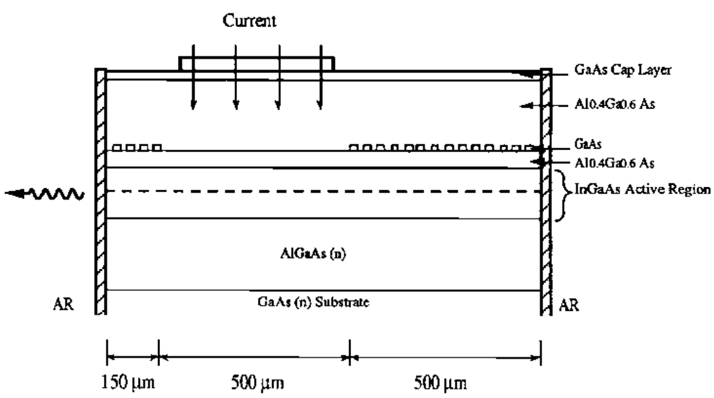

Fig. 13 Schematic diagram of the InGaAs DBR lasers. The front and rear grating lengths are 150 and 500 µm, respectively [24].

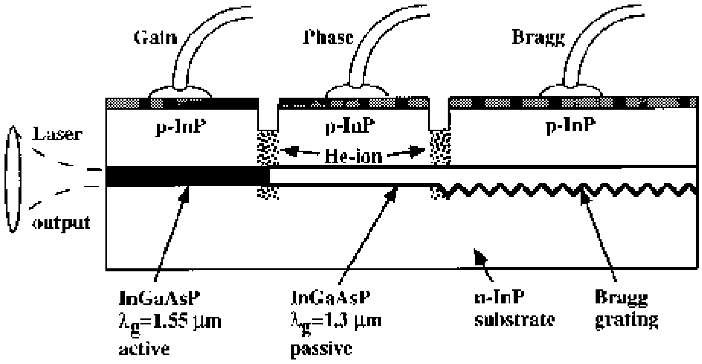

Fig. 14 Schematic of the three-section DBR laser structure [25].

A conventional DBR laser diode contains some corrugated waveguide structure (a grating section) providing wavelength-dependent feedback to define the emission wavelength. Another section of the laser waveguide acts as the amplifying medium (active region), and the other end of the resonator may have another DBR.

DBR laser diodes are usually single-frequency lasers with diffraction-limited output, and often they are wavelength-tunable (*tunable lasers*) Fig. 14. Tuning within the free spectral range of the laser resonator may be accomplished with a separate *phase section*, which can e.g. be electrically heated, or simply by varying the temperature of the gain region via the drive current. If the temperature of the whole device is varied, the wavelength response is significantly smaller than for an ordinary single-mode laser diode, since the reflection band of the grating is shifted less than the gain maximum. Electro-optic tuning can also be accomplished. Mode-hop free tuning over a larger wavelength region is possible by coordinated tuning of the Bragg grating and the gain structure.

There are more sophisticated device designs, exploiting a kind of Vernier effect with sampled gratings (***SG-DBR laser***), that offer a tuning range as wide as e.g. 40 nm, although not without mode hops.

The linewidth of a DBR diode is typically a few megahertz. Due to the relatively short laser resonator, it is larger than that e.g. of an external-cavity diode laser.

There are ***Master Oscillator Power Amplifier (MOPA) structures*** where an additional amplifier section (a semiconductor optical amplifier) is placed on the same semiconductor chip. The actual DBR laser is then the seed laser. Output powers above 10 W can be achieved with such devices [31].

Single mode strained-layer lasers [30] have been fabricated which use buried second order gratings for distributed Bragg reflectors. The lasers contain a strained GaInAs quantum well in the active region and operate in an edge emitting fashion with cw powers in excess of 110 mW. Single longitudinal and transverse mode operation is maintained at 971.9 nm up to 42 mW. Total power conversion efficiencies as high as 28% have been observed. The longitudinal and transverse mode behavior is stable under 90% amplitude modulation with 50% duty cycle pulses at 10 kHz and 10 MHz.

Applications of DBR laser diodes include optical fiber communications, free-space optical communications, laser cooling, optical metrology and sensors, and high-resolution spectroscopy. DBR lasers actually compete with external-cavity diode lasers (ECDLs), which also offer wavelength-tunable single-frequency output, with potentially better performance e.g. in terms of noise, but also requiring a significantly more complex setup. Chips containing DBR laser arrays can serve as very compact sources for use in wavelength division multiplexing systems.

Examples of special laser structures have been developed to achieve an improved beam quality are the ***tapered DFB lasers*** [32, 33, 34, 35, 36, 37], ***antiresonant reflecting optical waveguide (ARROW) laser*** [38], the ***alpha-DFB-laser*** [39, 40, 41, 42, 43, 44, 45]. The latter device allowed for nearly 1 W optical output power in a diffraction limited beam. Yet the fabrication of these devices proved to be very difficult due to the necessity of very precise grating structures and multiple etching and epitaxial growth steps.

There are ***tapered diode lasers***, having a region where the width and thus the area of the active region is significantly increased along the propagation direction. Due to a straight region with smaller width, the beam quality and brightness achieved are better than in a laser diode with the maximum width along the whole active region. However, the output exhibits strong astigmatism, which may depend on the operation power.

The dependence of the beam quality of **tapered laser** oscillators and amplifiers on the modal optical gain is demonstrated experimentally and theoretically for the first time. Tapered devices with high- (HMG) and low-modal gain (LMG) structures are compared in terms of output power and beam quality. At high-output powers the beam quality of LMG devices is by a factor of ten better than the beam quality of high-modal gain devices. The beam quality remains nearly unchanged up to power levels of more than 5-W continuous-wave (CW) where a beam quality factor of $M^2<3$ is achieved for both, tapered laser oscillators and tapered amplifiers .

A distributed Bragg reflector (DBR) tapered diode laser [37] (Fig. 15) with a record optical output power of 12 W and a conversion efficiency of about 44% is presented.

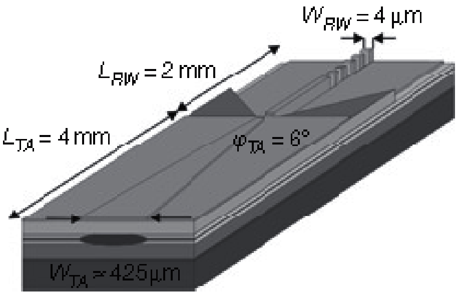

Fig. 15 Schematic three-dimensional view of DBR tapered laser

The device has a sixth-order surface grating and shows single longitudinal mode emission at 979 nm as well as a nearly diffraction limited beam. At 11.4 W the laser has a lateral beam propagation factor of M^2_{1/e^2} - 1.1 with 72% of the power in the central lobe.

In Ref. [44] a detailed experimental study of the far-field characteristics of mid-IR a-DFB lasers with W active regions was performed.

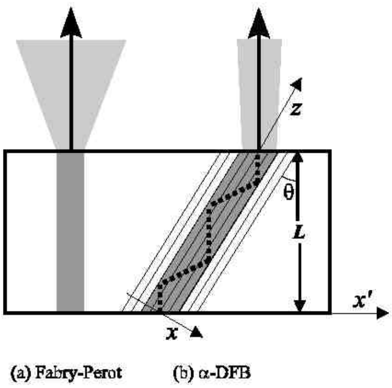

Fig. 16 Schematic views of (a) Fabry-Perot and (b) alfa-DFB lasers

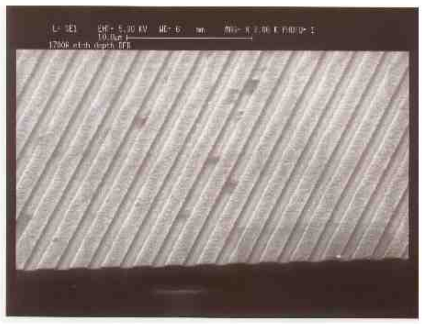

Fig. 17 Micrograph of the surface of an alfa-DFB laser with angled grating.

It is supposed in [45] that in the near future, only two types of broad-area single-spatial mode lasers will be commercially available: flared-amplifier (***tapered***) lasers and angled-grating distributed-feedback (**alfa-DFB**) lasers (Fig. 16, Fig. 17 and Fig. 18). Near-diffraction-limited powers of 5W and 1.6 W have been reported for these lasers, respectively.

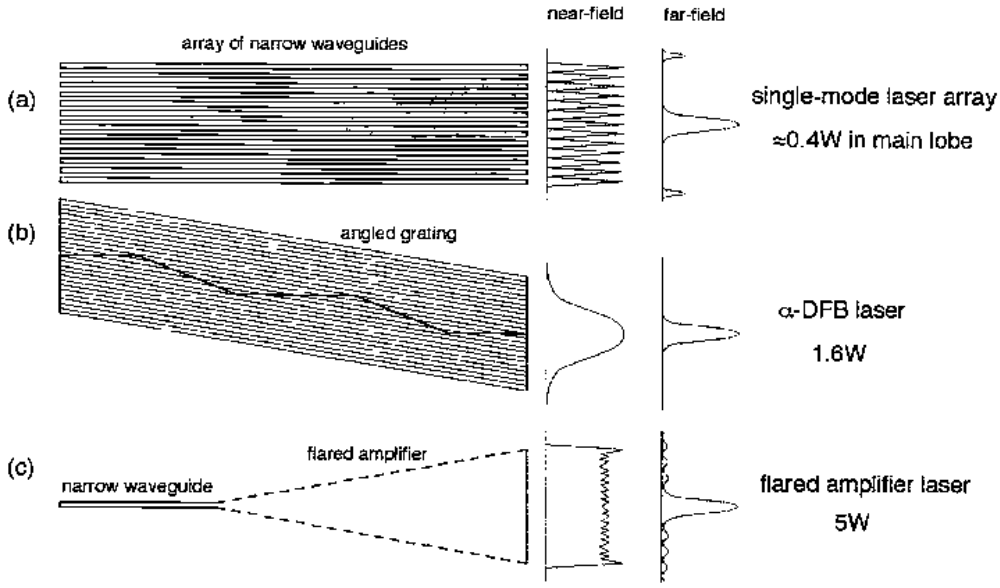

Fig. 18 Three types of high-brightness lasers; (a) mode-locked narrow-waveguide array, (b) a-DFB laser, (c) flared-amplifier laser.

In conclusion advantages of DBR, DFB lasers and their variations are accompanied by complex processing, low yield and high cost.

2. Diode External Cavity Lasers

An external-cavity diode laser [46, 47, 48, 49] is a semiconductor laser based on a laser diode chip which typically has one end anti-reflection coated, and the laser resonator is completed with, e.g., a collimating lens and an external mirror as shown in Fig. 19. Another type of external-cavity laser uses a resonator based on an optical fiber rather than on free-space optics. Narrowband optical feedback can then come from a fiber Bragg grating.

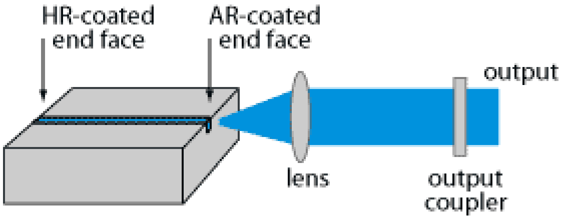

Fig. 19 Simple setup of a diode laser with external cavity. The semiconductor chip is anti-reflection coated on one side, and the laser resonator extends to the output coupler mirror on the right-hand side.

The external laser resonator introduces various new features and options:

- The longer resonator increases the damping time of the intracavity light and thus allows for lower phase noise and a smaller emission linewidth (in single-frequency operation). An intracavity filter such as the diffraction grating can further reduce the linewidth. Typical linewidths of external-cavity diode lasers are below 1MHz.

- Wavelength tuning is possible by including some adjustable optical filter as tuning element. Most often, a diffraction grating is used for this purpose. For details, see below.

Note that there are external-cavity semiconductor lasers, which, however, are usually not diode lasers: vertical external-cavity surface-emitting lasers (VECSELs).

Tunable external-cavity diode lasers (tunable lasers) usually use a diffraction grating as the wavelength-selective element in the external resonator. They are also called **grating-stabilized diode lasers**.

The common Littrow configuration (see Fig. 20a) contains a collimating lens and a diffraction grating as the end mirror. The first-order diffracted beam provides optical feedback to the laser diode chip, which has an anti-reflection coating on the right-hand side. The emission wavelength can be tuned by rotating the diffraction grating. A disadvantage is that this also changes the direction of the output beam, which is inconvenient for many applications.

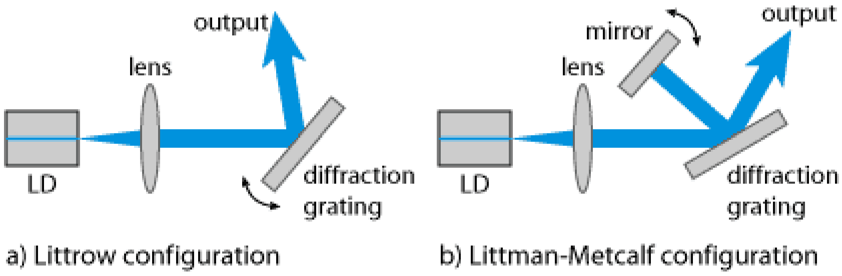

Fig. 20 Tunable external-cavity diode lasers in Littrow and Littman–Metcalf configuration.

In the Littman–Metcalf configuration ([33], Fig. 20b), the grating orientation is fixed, and an additional mirror is used to reflect the first-order beam back to the laser diode. The wavelength can be tuned by rotating that mirror. This configuration offers a fixed direction of the output beam, and also tends to exhibit a smaller linewidth, as the wavelength selectivity is stronger. (The wavelength-dependent diffraction occurs twice instead of once per resonator round trip.) A disadvantage is that the zero-order reflection of the beam reflected by the tuning mirror is lost, so that the output power is lower than that for a Littrow laser.

Note that the mechanical stability of external cavity lasers, however, is a critical point since the mirror (grating) is not integrated on the wafer. Consequently, lasers with external mirrors (gratings) are expensive devices.

3. Diode Lasers with the all-epitaxial design

Recently concepts of Tilted Cavity Laser (TCL, [5, 50, 51, 52]) and Tilted Wave Laser (TWL, [6]) were proposed. The concept of wavelength stabilization in edge–emitting lasers, which is achieved exclusively through epitaxial design is discussed in [5]. The idea based on the existence of the leaky tilted modes originating in planar waveguides with thin cladding layers. The basic principles of the concept are described in the part **2. Tilted wave laser (TWL) concept.** The light of these modes is propagating at the leakage angle outside the waveguide and is being reflected back, for example, by a Bragg multilayer structure, which is designed to provide a maximum reflectivity at this tilt angle (TCL construction). Once the average refractive indices of the sections are different, the law of refraction makes the related resonance wavelengths to match only at fixed angle(s) and, thus, wavelength(s).

As it was already mentioned above, in the case of TCL, the wavelength stabilization is based on the narrow stopband of the resonance multilayer reflector. The intersection of the cavity and the reflector in the angle space results in a narrow spectral range, where the leakage loss is small [51, 52]. The light, which is not at the minimum loss wavelength is absorbed or scattered in the substrate and cannot contribute to lasing.

In the second approach – TWL – [6], no leakage loss selectivity is necessary and the wavelength stabilization is realized through phase matching, which occurs only in case of lasing or at least stimulated emission in the device. All the leaky light is reflected in this approach back to the cavity by a single (or multiple) reflection from the underlying layer (layers). Coherent leaky light, passing through multiple reflections accumulates a phase difference and interferes with the light, which is propagating in the planar leaky waveguide. In case the interference is constructive, the phase matching condition is fulfilled and wavelength stabilization is taking place. The easiest approach to realize such a device is to use the back reflection of the leakage emission from the polished substrate backside towards the active zone of the leaky waveguide.

On-wafer etching may enable on-chip DFB-class multi-wavelength arrays. The TWL approach thus provides an opportunity to reduce costs of the device in comparison with TCL due to a simpler, thinner and much more robust layer architecture.

One more advantage of the TWL concept is the fact that the vertically-integrated electro-optical modulator (EOM) concept could be easily applied to such a laser. The all-epitaxial coupled cavity edge-emitting EOM TWL will operate in such a way that only one cavity will serve as an exit cavity (the EOM cavity). The second cavity (the TWL cavity) will operate in a high-order vertical mode with an effective mode angle beyond the angle of the total internal reflection at the facet surface. EO modulation of the coupling strength between the two cavities will modulate the output power.

Thus, combination of the wavelength stabilization and EO modulation approach provides a key synergetic advantage and enables a new generation of ultrahigh-speed edge-emitters.

A schematic approach of possible integration of the TWL laser and EO modulator is presented in Fig. 21. The mode tilt angle is chosen to be beyond the angle of the total internal reflection. Thus, no light can come out of the waveguide. For light outcoupling an additional narrow waveguide is epitaxially integrated into the structure, to enable a small fraction of the light to undergo a diffraction outcoupling through this layer (Fig. 16). The coupling strength between the thin waveguide and the TWL section is controlled by the EO-modulator media, which is introduced either directly into the narrow coupled waveguide, or adjusted in its vicinity. Now the coupling efficiency can be tuned and the EO-modulated TWL can be realized.

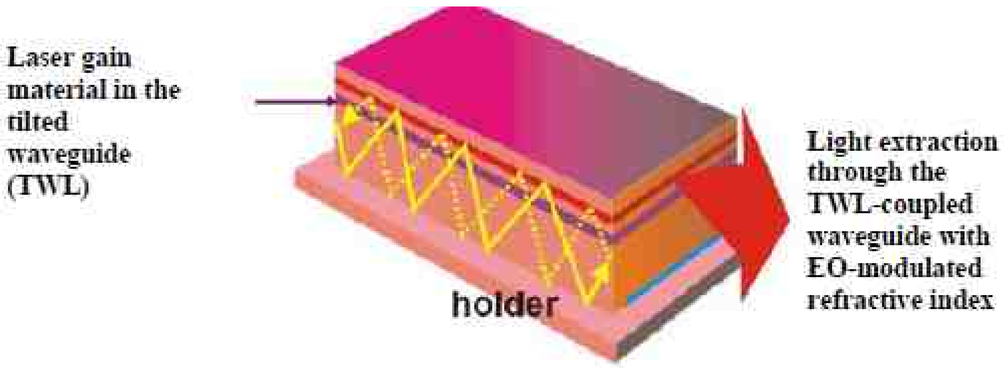

Fig. 21 Tilted wave laser with the light outcoupling through the EO-modulated waveguide layer.

The EOM TWL devices will be targeting 1300 nm wavelength to address applications in medium range LAN and access networks (RoF, PON).

III. Comparison

The Tilted Wave Laser (TWL) concept bridges the gap, being comparable in cost to VCSELs. On one side it provides the performance characteristic of DFB devices. On the other side it can be easily integrated vertically with the EO modulator section and, thus, operate at ultrahigh speeds. There are two key features, which enable the functionality of the EOM TWL:

1) Single wavelength operation and wavelength stabilization

The all epitaxial TWL design enables single-wavelength-stabilized operation, which is a must both for proper single mode single wavelength DFB-class operation, needed for coupling to single mode fiber and avoiding wavelength dispersion effects, and also a prerequisite for intensity modulation using the electro-optical effect.

The key advantage of the proposed concept is all epitaxial design, which significantly reduces production costs. In all other single-wavelength-stabilized approaches complicated processing or complicated external cavity construction are required.

2) Possibility of vertical Integration

Applying the concept of high-order "tilted" mode gives an opportunity to couple vertically the two key sections of the device: the TWL section, providing wavelength-stabilized lasing and operating at a mode angle beyond the angle of the total internal reflection at the facet, and the light output section, which enables light outcoupling through a facet, where the coupling efficiency of this section is electro-optically controlled through the refractive index modulation.

References

---

1 Mitsuo Fukuda, Optical Semiconductor Devices, John Wiley & Sons, New York, 1999.

2 S.A.Blokhin, A.V.Sakharov, N.A.Maleev, M.M.Kulagina, Yu.M.Shernyakov, I.I.Novikov, N.Yu.Gordeev, M.V.Maximov, A.G.Kuzmenkov, V.M.Ustinov, N.N.Ledentsov, A.R.Kovsh, S.S.Mikhrin, G.Lin, J.Y.Chi, The impact of thermal effects on the performance of vertical-cavity surface-emitting lasers based on sub-monolayer InGaAs quantum dots, Semiconductor Science and Technology, 22 (3), 203 (2007).

3 V.I.Shveikin, V.A.Gelovani, New diode lasers with leaking emission in an optical cavity Quantum Electronics 32(8) 683-688 (2002).

4 D.R.Scrifers, W.Streifer, R.D.Burnham, Appl. Phys. Lett., 29, 23 (1976).

5 N.N.Ledentsov and V.A.Shchukin, Novel concepts for injection lasers, Optical Engineering 41 (12), 3193 (2002).

6 N.N.Ledentsov, V.A.Shchukin and D.Bimberg, "Merging Nanoepitaxy and Nanophotonics", In Future Trends in Microelectronics. Up the Nano Creek, S. Luruy, J. Xu and A. Zaslavsky, Eds. John Wiley and Sons Inc., 2007, pp. 401-- 431

7 J.Berenger, A perfectly matched layer for the absorption of electromagnetic waves, Journal of Computational Physics, 114, 185 (1994).

8 S.G.Johnson, Notes on Perfectly Matched Layers, online MIT course notes. http://math.mit.edu/~stevenj/18.369/ (2007).

9 J.Mielewski, M.Mrozowski, Application of the Arnoldi method in FEM analysis of waveguides. Microwave and Guided Wave Letters, 8(1), 7 (1998).

10 S.Adachi, J. Appl. Phys., 58(3), (1985)

11 J.S.Roberts, G.H.Scott, J.Gowers, Structural and photoluminescent properties of GaxIn1−xP(x[approximately-equal-to]0.5) grown on GaAs by molecular beam epitaxy,: J. Appl . Phys. 52 (1981) 4018.

12 M.A.Afromowitz, Refractive indexes of Ga1-xAlxAs, Solid State Communications, 15, 59 (1974).

13 V.I.Shveikin, A.P.Bogatov, A.E.Drakin, Yu.V.Kurnyavko, Angular distribution of the radiation from quantum-well `leaky-wave' InGaAs/GaAs lasers, Quantum Electronics 29 (1), 33 (1999).

14 N.M.Lyndin, V.A.Sychugov, and B.A.Usievich, Spectral selectivity of radiation- and tunnel-coupled waveguide structures, Zh. Tekh. Fiz. 67, 59 (1997).

15 H. Kogelnik and C. V. Shank, “Coupled-wave theory of distributed feedback lasers”, J. Appl. Phys. 43 (5), 2327 (1972).

16 A.Yariv, Coupled-mode theory for guided-wave optics, IEEE J. Quantum Electron. QE-9, 919 (1973).

17 D. A. Ackerman, L. M. Zhang, P. A. Morton, G. E. Shtengel and J. A. Sheridant, “Real-world distributed feedback lasers- measured, modeled and applied to CATV”, SPIE 2693, 600 (1996)

18 T.R. Chen, Nong Chen, Wei Hsin, Steven Chen, Paul Chen, “Ultra-wide temperature range operation of DFB lasers at 1310 nm and 1490 nm”, SPIE 7135 (2008)

19 J. Koeth, M. Fischer, M. Legge, J. Seufert, R. Werner, “High Performance Quantum Dot Distributed Feedback Laser Diodes around 1.15 mkm” SPIE 6909 (2008)

20 K. Sato, “Chirp characteristics of 40-Gb/s directly modulated distributed-feedback laser diodes”, IEEE J. Lightwave Technol. 23 (11), 3790 (2005)

21 A. Schülzgen et al., “Distributed feedback fiber laser pumped by multimode laser diodes”, Opt. Lett. 33 (6), 614 (2008)

22 R. D. Dupuis and E. P. Dapkus, “Room-temperature operation of distributed-Bragg-confinement Ga1−xAlxAs-GaAs lasers grown by metalorganic chemical vapor deposition”, Appl. Phys. Lett. 33 (1), 68 (1978)

23 M.-C. Amann et al., “Tunable twin-guide laser: a novel laser diode with improved tuning performance”, Appl. Phys. Lett. 54, 2532 (1989)

24 S. O'Brien, R. Parke, D. F. Welch, D. Mehuys and D. Scifres, ”High power GaInAs QW lasers with distributed Bragg reflectors”, SPIE 1634, 329 (1992)

25 Anders P. Larson, Lars Sandstrm, Svante Hojer, Henrik Ahlberg, Bjorn Broberg, “Evaluation of distributed Bragg reflector lasers for high-sensitivity near-infrared gas analysis”, Opt. Eng. 36(1) 117 (1997)

26 G. Morthier et al., “A λ/4-shifted sampled or superstructure grating widely tunable twin-guide laser”, IEEE Photon. Technol. Lett. 13 (10), 1052 (2001)

27 L. A. Coldren et al., “Tunable semiconductor lasers: a tutorial”, J. Lightwave Technol. 22 (1), 193 (2004)

28 R. Todt et al., “Wide wavelength tuning of sampled grating tunable twin-guide laser diodes”, Electron. Lett. 40, 1491 (2004)

29 R. Todt et al., “Sampled grating tunable twin-guide laser diodes with over 40-nm electronic tuning range”, IEEE Photon. Technol. Lett. 17 (12), 2514 (2005)

30 S. O'Brien, R. Parke, D. F. Welch, D. Mehuys and D. Scifres “High power GaInAs QW lasers with distributed Bragg reflectors”, SPIE 1634, 329 (1992)

31 H.Wenzel, K.Paschke, O.Brox, F.Bugge, J.Fricke, A.Ginolas, A.Knauer, P.Ressel, G.Erbert, “10W continuous-wave monolithically integrated master-oscillator power-amplifier”, Electronics Letters 43 (3), 160 (2007)

32 J. N. Walpole, "Semiconductor amplifiers and lasers with tapered gain regions", Opt. Quantum Electron. 28 (6), 623 (1996)

33 M. Mikulla et al., "High-brightness tapered semiconductor laser oscillators and amplifiers with low-modal gain epilayer structures", IEEE Phot. Tech. Lett. 10 (5), 654 (1998)

34 M. Krakowski, S.C. Auzanneau, F. Berlie, M. Calligaro, Y. Robert, O. Parillaud and M. Lecomte, “1W high brightness index guided tapered lasers”, Electronics Letters 39 (15), (2003)

35 B. Sumpf, R. Hulsewede, G. Erbert, C. Dzionk, J. Fricke, A. Knauer, W. Pittroff, P. Ressel, J. Sebastian, H. Wenzel and G. Trankle “High-brightness 735nm tapered diode lasers”, Electronics Letters 38 (4), (2002)

36 M.T. Kelemen, J.Weber, G. Kaufel, G. Bihlmann, R. Moritz, M. Mikulla and G. Weimann, “Tapered diode lasers at 976nm with 8W“, Electronics Letters 41 (18), (2005)

37 C. Fiebig, G. Blume, C. Kaspari, D. Feise, J. Fricke,M. Matalla, W. John, H. Wenzel, K. Paschke and G. Erbert, ”12W high-brightness single-frequency DBR tappered laser”, Electronics Letters 44 (21), (2008)

38 C. Zmudzinski et all, "Three-core arrow-type diode laser: novel high-power, single-mode device, and effective master oscillator for flared antiguided mopas", IEEE J.Sel. Topics Quant. Electron. 1 (2), 129 (1995)

39 A. M. Sarangan et al., "Spectral properties of angled grating high-power semiconductor lasers", IEEE J. Quantum Electron. 25 (8), 1220 (1999)

40 A.P.Bogatov, A.E.Drakin, D.V.Batrak, R. Guther, K.Paschke, H.Wenzel, Spectral properties of a semiconductor a-DFB laser cavity, Quantum Electronics 36 (8) 745 (2006).

41 K. Paschke, R. Guther, J. Fricke, F. Bugge, G. Erbert and G. Trankle, “High power and high spectral brightness in 1060nm a-DFB lasers with long resonators”, Electronics Letters 39 (4), (2003)

42 R. J. Lang, K. Dzurko, A. A. Hardy, S. DeMars, A. Schoenfelder, and D. F. Welch, “Theory of grating-confined broad-area lasers”, IEEE J. Quantum Electron. 34, 2196 (1998)

43 A. M. Sarangan, M. W. Wright, J. R. Marciante, and D. J. Bossert, “Spectral properties of angled-grating high-power semiconductor lasers”, IEEE J. Quantum Electron. 35, 1220 (1999)

44 W. W. Bewley, I. Vurgaftman, R. E. Bartolo, M. J. Jurkovic, C. L. Felix, and J. R. Meyer H. Lee and R. U. Martinelli G. W. Turner and M. J. Manfra, “Beam Quality of Mid-Infrared Angled-Grating Distributed-Feedback Lasers”, SPIE 4287 (2001)

45 Mats Hagberg, Steve OBriena, Bardia Pezeshki, Ed Veil, Bo Lu, Robert Lang, ”High-brightness flared lasers”, SPIE 3628 (1999)

46 M. G. Littman and H. J. Metcalf, “Spectrally narrow pulsed dye laser without beam expander”, Appl. Opt. 17 (14), 2224 (1978)

47 K. Liu and M. G. Littman, “Novel geometry for single-mode scanning of tunable lasers”, Opt. Lett. 6 (3), 117 (1981)

48 M. Fleming and A. Mooradian, “Spectral characteristics of external-cavity controlled semiconductor lasers”, IEEE J. Quantum Electron. 17 (1), 44 (1981)

49 C.J.Hawthorn et al., “Littrow configuration tunable external cavity diode laser with fixed direction output beam”, Rev. Sci. Instrum. 72 (12), 4477 (2001)

50 N.N.Ledentsov, V.A.Shchukin, A.R.Kovsh, S.S.Mikhrin, I.L.Krestnikov, A.V.Kozhukhov, N.Y.Gordeev, L.Ya.Karachinsky, M.V.Maximov, I.I.Novikov, and Yu.M.Shernyakov, “Edge and surface-emitting tilted cavity lasers”, SPIE Photonics West 2005 International Symposium, January 22–27, 2005, San Jose, California, USA, Proceedings of SPIE, Volume 5722, pp. 130-146 (2005)

51 V.A.Shchukin, N.N.Ledentsov, L.Ya.Karachinsky, I.I.Novikov, Yu.M.Shernyakov, N.Yu.Gordeev, M.V.Maximov, M.B.Lifshits, A.V.Savelyev, A.R.Kovsh, I.L.Krestnikov, S.S.Mikhrin, and D.Bimberg, ”High–power 975 nm tilted cavity laser with a 0.13 nm/K thermal shift of the lasing wavelength”, Semiconductor Science and Technology, 22 (9), 1061 (2007)

52 L.Ya.Karachinsky, I.I.Novikov, G.Fiol, M.Kuntz, Yu.M.Shernyakov, N.Yu.Gordeev, M.V.Maximov, M.B.Lifshits, T.Kettler, K.Posilovic, V.A.Shchukin, N.N.Ledentsov, S.S.Mikhrin, and D.Bimberg, “Tilted Cavity Concept for the High-Power Wavelength Stabilized Diode Lasers”, Proceedings of SPIE 7138, 713804-1 (2008)